OE Optical Engineering

RESEARCH PAPER

Automation and miniaturization of optometry instrument based on the ANSI/ISEA Z87.1 standard

Cheng-Chung Lee,[a] Ching-Huang Lin,[b] Tai-Chuan Ko,[a] and Chun-Feng Su[a,*]

[a]National Yunlin University of Science and Technology, Graduate School of Engineering Science and Technology, Yunlin, Taiwan

[b]National Yunlin University of Science and Technology, Department of Electronic Engineering, Yunlin, Taiwan

ABSTRACT. The current measurement equipment, which adheres to the ANSI Z87.1 standard measurement method, features an extended path length of nearly 11 m. This extended length poses challenges for laboratories or testing units in terms of space utilization and significantly impacts the energy configuration required for accurate detection. The initial phase of this study focuses on automation, entailing the development of a measuring device equipped with full automation capabilities. This device ensures the precise measurement of diopter and astigmatism data at a consistent and efficient pace. The subsequent phase aims to minimize the distance between the objective lens and the target without altering the fundamental principles of the original diopter testing system. This reduction is achieved through the utilization of optometry automatic detection technology. Concurrently, to complement the scaled-down detection equipment, precision optical targets are manufactured using semiconductor standard photomask fabrication techniques. Results indicate a substantial reduction in equipment size to <1 m, retaining the same level of precision. This reduction significantly economizes the installation space required for the instrument. The implementation of automated measurements minimizes errors stemming from human judgment and allows the device to be employed in the assessment of various safety lenses.

© The Authors. Published by SPIE under a Creative Commons Attribution 4.0 International License. Distribution or reproduction of this work in whole or in part requires full attribution of the original publication, including its DOI. [DOI: 10.1117/1.OE.63.2.024106]

Keywords: optometry; automation; miniaturization; semiconductor standard process; standard optic measurement

Paper 20230599G received Jun. 18, 2023; revised Jan. 14, 2024; accepted Jan. 28, 2024; published Feb. 16, 2024.

1 Introduction

Plano lenses, whether with the convex side facing the eye or the concave side toward it, are notably useful for spectacle testing through neutralization, being adaptable to various forms.[1] Lenses with zero diopter, commonly referred to as plano lenses, find widespread use in specialized eyewear, including sunglasses, sports glasses, snow goggles, safety glasses, goggles, and masks. These serve the dual purpose of eye protection, facial covering, and aesthetic appeal, holding a significant position in the global market each year. In 2020, the global market size for safety glasses amounted to US$ 1686.98 million, projected to reach US$ 1692.16 million by 2027, indicating a growth rate of 1.80% between 2021 and 2027.[2] Additionally, the global sports sunglasses market achieved a value of US$ 2.9 billion in 2021. The IMARC Group anticipates this market to escalate to US$ 3.7 billion by 2027, demonstrating a compound annual growth rate (CAGR) of 4.07% from 2022 to 2027.[3] The testing of plano lenses necessitates the assessment of diopter and astigmatism, requiring adherence to a specified tolerance range.

*Address all correspondence to Chun-Feng Su, sp1966f@gmail.com

The design of such measuring instruments must align with the standards outlined in section 9.4 of ANSI Z87.1-2020,[4] which details the test requirements for diopter, astigmatism, clarity, is an American National Standard used for safety purposes such as safety glasses, safety goggles, side shields, and other eye and face protection devices. The industry benchmark for eye and face protectors has undergone six revisions and has been incorporated into regulatory guidelines by the U.S. Occupational Safety and Health Administration. These regulations mandate employers to provide appropriate safety glasses and face protectors. However, existing measuring instruments with optical components meeting these specifications often feature elongated and narrow path lengths, resulting in inefficient utilization of space within the instrument configuration. This setup restricts the intervention of personnel or objects during the measurement process. Practical laboratory planning frequently encounters challenges where available space is insufficient, leading to wasted or inefficiently used areas. Over recent years, advancements in semiconductor manufacturing processes and photonic technology have led to the transformation of cumbersome laboratory instruments into compact, field-deployable devices.[5,6] With the rapid evolution of technology and the increasing demand for high-quality, low-defect-rate products, the importance of automatic optical inspection (AOI) technology has amplified. AOI technology is intelligent, flexible, and yields more consistent results compared to manual visual inspection.[7] It is considered robust and capable of replacing human inspectors who may experience fatigue and monotony during inspection tasks.[8]

Recognizing the efficiency and increased accuracy of automated techniques compared to manual estimations,[9,10] this study embarked on refining an advanced optical inspection (AOI) design and developing a sample fixture-based measurement mechanism. The primary goal was to substantially reduce manpower needs and operational measurement times. Moreover, considerable efforts were made to downsize the machine, reducing installation space requirements while ensuring maintained inspection quality. We anticipate that these advancements will not only contribute to the field of advanced optical inspection (AOI) but also serve as a valuable reference for informing future revisions of ANSI Z87.1.

2 Existing Techniques

2.1 Optical Inspection Techniques

Optical inspection techniques can be broadly categorized into two primary types: manual optical inspection, conducted by human inspectors, and AOI, which utilizes an image sensor and processor.[9] As per section 9.4 of ANSI Z87.1-2020, the calibration layout for diopter and astigmatism in optometry instruments should include an eyepiece, manual focusing mechanism, telescope, lens fixtures, and a light box for pattern testing. The apparatus should feature an eight-power calibrated telescope (preferably equipped with a reticle), with a minimum aperture of 19 mm (0.75 in.) for plano-spherical lenses and 7 mm (0.28 in.) for plano-toric or plano-aspheric lenses. It should also include a fixture to hold the protector in the test position and a combined sunburst and resolution test pattern.

The test pattern, featuring the sunburst lines with resolution patterns (Fig. 1), should be positioned at a distance of 10.67 m (35 ft) from the telescope's objective lens and should be adequately illuminated, either backlit or by other means, to conduct the test effectively (Fig. 2). The telescope comprises the eyepiece F1, the objective lens F2, and the focal length adjustment mechanism. In the absence of a sample, when the target is clearly visible, the distance between the eyepiece F1 and the objective lens F2 is "D," and the distance between the objective lens and the target is "d." Upon placing the sample T3, the image of the target becomes unclear. At this point, adjusting the distance "D" between F1 and F2 makes the target visible again, resulting in a variation denoted as "δ."

The "YT-306 Telescope Optical Tester (US Standard) - Plano Eyewear Dioptometer" used in this study is manufactured by the Yin-Tsung Company and meets the specified specifications.[11] Figures 3(a) & 3(b) showcase the telescope, which is equipped with an adjustment mechanism, and the target, featuring a light box.

2.2 Manual Optical Inspection

Within the diopter test system, the operator modifies the focal length of the telescope to assess the clarity of a distant target. When a lens sample is positioned in front of the telescope, a spherical

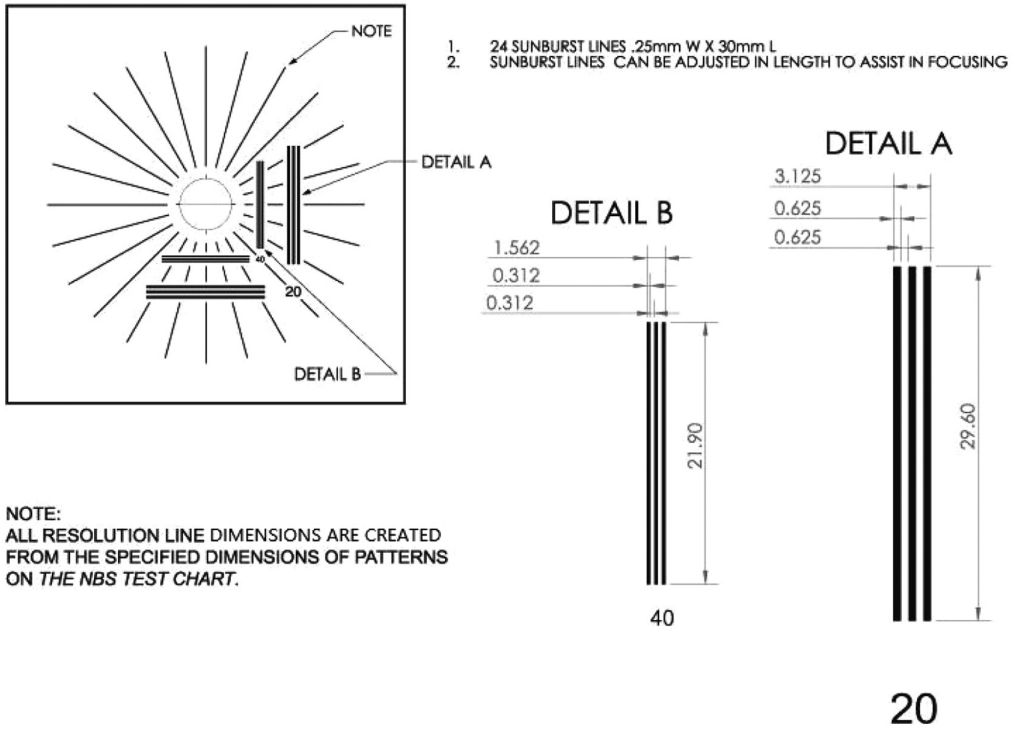

Fig. 1 The test resolution pattern with a radial sunburst power target superimposed according to ANSI Z87.1-9.4.

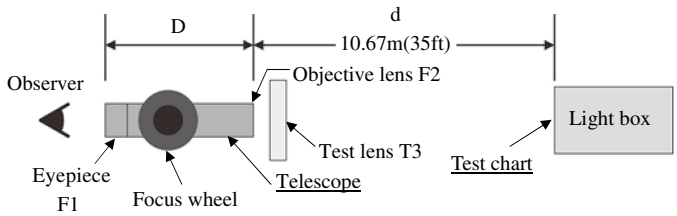

Fig. 2 Schematic of the calibration instrument designed for optometry applications in accordance with the ANSI/ISEA Z87.1-2020 standard.

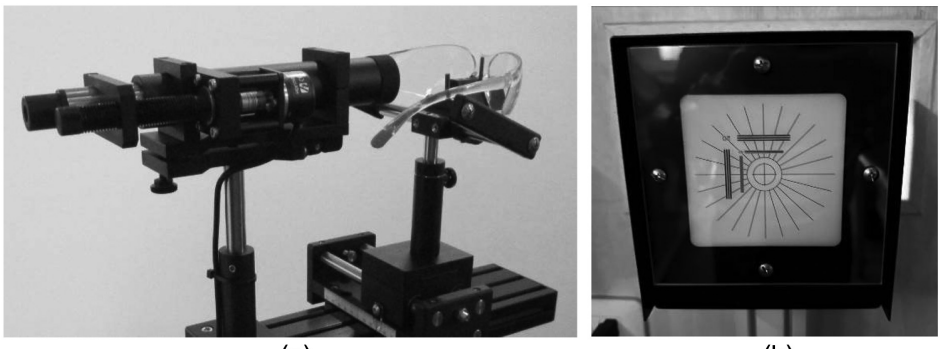

Fig. 3 (a) Part of the diopter testing system and (b) target with backlight.

lens will reveal only one distinct target, as depicted in Fig. 4(a). Conversely, astigmatism will display two clear targets—D1 and D2, showcased in Figs. 4(b) & 4(c), calculated in accordance with Z87.1-9.4.3[12] as follows:

$$\text{Diopters}: \frac{(D1 + D2)}{2}, \ (\text{standard range } \pm 0.06D), \tag{1}$$

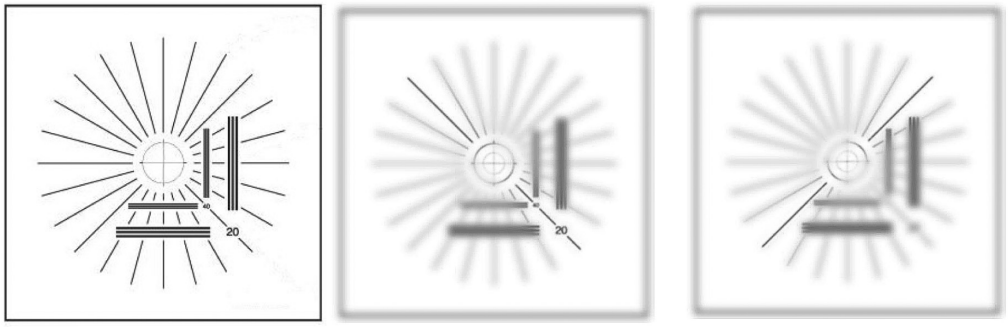

Fig. 4 Graphics at different focal lengths for Z87.1-2020 (a) without astigmatism, (b) clear D1 image at 135 deg, and (c) clear D2 image at 45 deg.

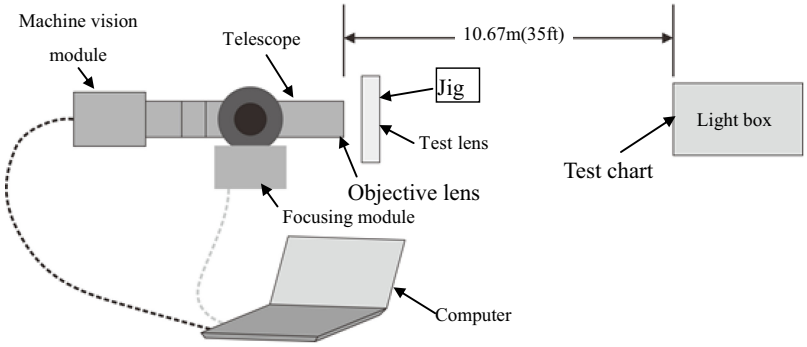

Fig. 5 System architecture of optometry automatic detection instrument.

$$\text{Astigmatism Power: } |\text{D1} - \text{D2}|, \ (\text{standard range } 0.06\text{D}). \tag{2}$$

2.3 Original Automatic Optical Inspection

The initial AOI method involved visual observation and manual focus to compute the diopter and astigmatism, illustrated in Fig. 5.

Computer vision technology is extensively applied across numerous practical domains today, encompassing optical character recognition, machine inspection, retail, 3D model construction (photogrammetry), medical imaging, automotive safety, match move, motion capture (mocap), surveillance, fingerprint recognition, and biometrics, among others.[13]

In this study, we adhere to the principles of AOI techniques as established in "optometry automatic detection technology."[14] We employ computer vision through the use of cameras and auto-focus modules, substituting human visual observation and manual focus with machine vision and computer-controlled focus mechanisms. This transition enhances detection speed and reduces measurement discrepancies.

3 Methods

3.1 Architecture Design

To achieve system miniaturization and automatic measurement while adhering to the 8× telescope requirements outlined in Article 9.4 of ANSI Z87.1-2020, this study reduced the distance from the largest objective lens to the target in the diopter test system (Fig. 2) to <1 m. Additionally, to maintain the system architecture of the optometry automatic tester (Fig. 5) within the constraints of producible target graphics, a new organizational design was implemented, integrating the test process. In the future, if ANSI Z87.1 incorporates the results of this experiment, further reduction in distance can be pursued through the implementation of a more robust optical system.

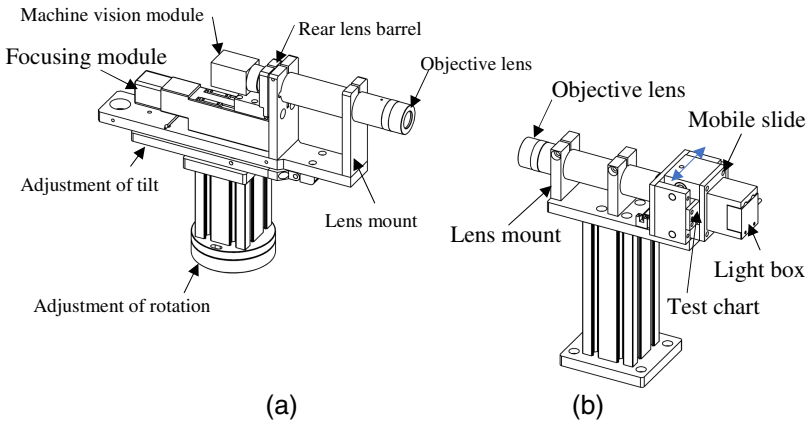

Fig. 6 (a) Telescope group and (b) target group.

3.2 Improvement of Original AOI

3.2.1 *Telescope group and target group*

The AOI telescope's design incorporates an automatic focusing feature. This mechanism involves securing the front lens and utilizing a stepping motor to move the slide, thereby adjusting the position of the rear lens barrel (camera) to change the focal length. The camera captures a contrast image, systematically scanning at fixed intervals to determine the optimal focus position's potential range. Subsequently, the computer calculates the position with the highest contrast, facilitating automatic focus adjustment.

For proper alignment with the optical axis of the target group, the telescope assembly requires a structure capable of tilting up and down and rotating left and right on the mounting base, as depicted in Fig. 6(a), allowing adjustment of the telescope's orientation. To prevent potential errors in computer judgment, the sunburst pattern for diopter and astigmatism measurement and the fringe pattern for sharpness measurement have been divided into separate left and right targets. Consequently, the target device necessitates lateral movement capability. To address this, a stepping motor controls the sliding table, which acts as a switching platform securely holding the high-precision reduced optical target. This setup involves placing a lens in front of the target to establish a parallel optical path with the telescope lens, significantly reducing the distance. Additionally, the light source is positioned behind the target, as illustrated in Fig. 6(b).

3.2.2 *Jig platform*

To meet the diverse requirements for measuring different samples, the use of various fixture types is necessary. For instance, when evaluating glasses as a single unit, a fixture for placing and adjusting the glasses, depicted in Fig. 7(a), is utilized. Alternatively, a separate fixture, shown in Fig. 7(c) and designed to position samples on a model resembling the human head, is employed.

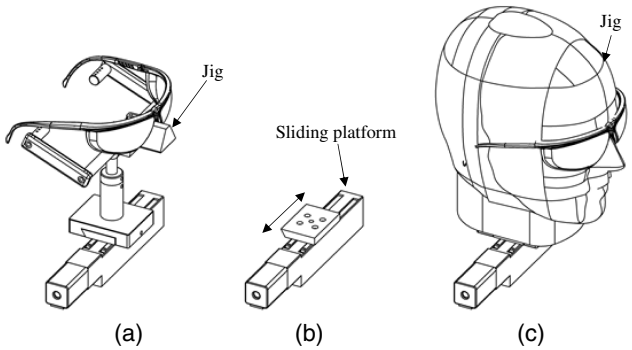

Fig. 7 Jig platform (a) Glasses jig, (b) mobile sliding platform, and (c) human head jig.

Because the device operates with a single optical path, scenarios that require separate measurements for left and right eyes necessitate an automatic adjustment of the sample position. To achieve comprehensive automation in measurement procedures, a sliding table controlled by a stepping motor, functioning as a switching platform, as illustrated in Fig. 7(b), is employed. Once the desired measurement position is set, this mechanism automatically shifts between the left and right eye positions, ensuring more precise measurement data and expediting the process.

3.3 Target Making

3.3.1 *Estimation of target scale*

Applying the thin lens imaging formula: $1/|p| + 1/|q| = 1/f$, and calculating the imaging magnification: $m = h'/h = q/p$, as represented in Fig. 8(a), provides the basis for further analysis.

By utilizing the target size from the initial specification,[6] the magnification is determined: $m = h'/h = q/p = 0.24/10.67 = 0.02249$. Therefore, the camera's target imaging size is reduced to 0.02249 times, as illustrated in Fig. 8(b).

To maintain the target imaging size ratio of the new structure to that of the original structure (both at a ratio of 0.02249), an additional lens with the same focal length as the original structure is needed in front of the target, as shown in Fig. 8(c), denoting $h' = h_1$.

3.3.2 *Reduced production of new target*

In this research, the necessity to significantly reduce the measurement distance also requires a proportional reduction in the target size. Specifically, the measurement distance is diminished from the original standard of 10.67 to 0.24 m, and consequently, the target size must be reduced by the ratio of 0.02249. This reduced target size poses a challenge as the minimum line width of the target pattern shrinks from 0.25 mm (h) to 0.0056225 mm (h1) = 5.6225 μm after applying the reduction ratio of 0.02249. Conventional printing technologies are incapable of producing such minute line widths. As a result, the only viable solution is to utilize mask manufacturing technology adhering to the semiconductor standard process to create a precision optical target.

A photo-mask substrate typically consists of a 6 in.^{2} sheet (~152 mm^2) sheet of fused silica. During photolithography, this substrate is adorned with a pattern of opaque and transparent areas

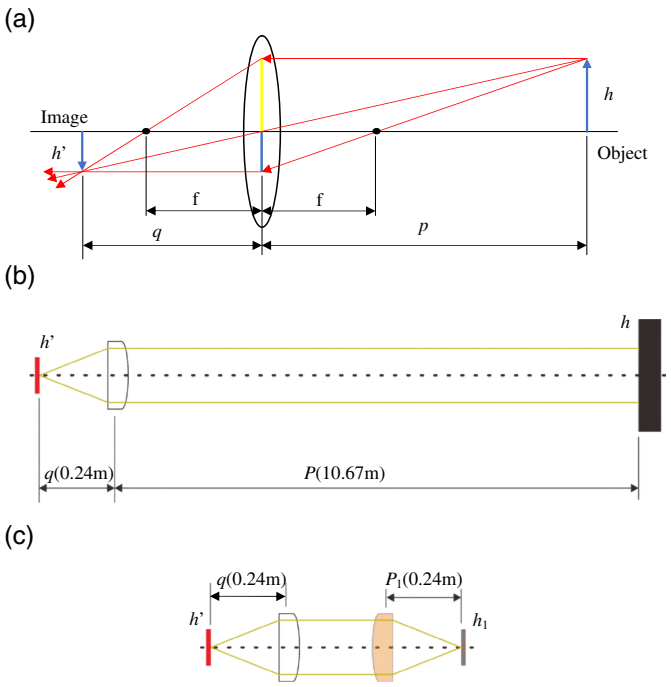

Fig. 8 (a) Imaging principle of thin lens, (b) imaging map of the original structure, and (c) imaging map of the target in this study.

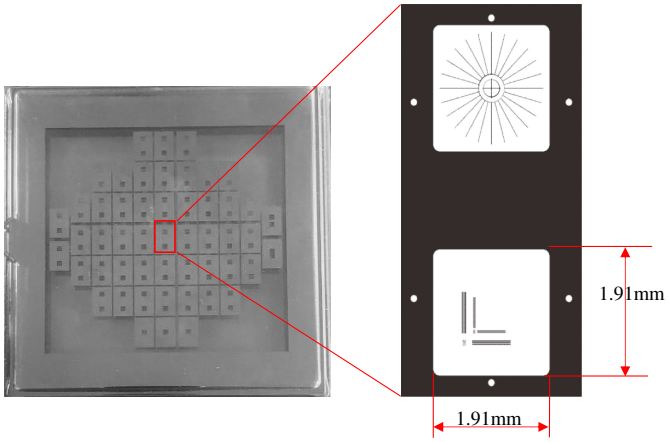

Fig. 9 (a) Complete finished photomask and (b) photomask design used in the radial sunburst image and clear line image.

that are projected onto the substrate. In the subsequent patterning step, numerous continuous pattern designs guide the material deposition or removal on the substrate. Finally, the completed pattern is cut out for use, as depicted in Fig. 9.

3.3.3 *Optical path adjustment*

To begin, secure the target holder and position its objective lens at a distance of 0.24 m from the target pattern [p1 in Fig. 8(c)]. Subsequently, fix the telescope assembly at an appropriate distance ensuring the transmission of parallel light within this range, a distance dictated by the fixture platform to accommodate the placement of test samples. Following this, adjust the distance between the telescope's objective lens and the camera to 0.24 m [q in Fig. 8(c)]. Using the image relayed by the camera, make further adjustments involving tilting up and down as well as rotating left and right to finely calibrate the orientation of the telescope assembly. This adjustment is crucial to ensure complete image capture by the camera.

4 Verification and Results

Two experiments are conducted in this study to validate the accuracy and adherence to the specifications of the newly designed system. In the first experiment, the study employed the new architectural design and utilized six standard diopter test lenses calibrated by the National Physical Laboratory (NPL), as indicated in their certificate of calibration for six test lenses and two prisms dated 2022 (Table 1). The intention was to utilize these test lenses in the measurement process.

Table 1 Lens specifications.

Identification	Measured power (diopters)	Test aperture (mm)	Center thickness (mm)	Curvature radius R1 (mm)	Curvature radius R2 (mm)	Glass material
D+0.050	+0.050±0.002	30	8	−201.9	−200	BK7
D+0.132	+0.132±0.002	30	8	−206.9	−200	BK7
D+0.257	+0.258±0.002	30	8	−218.4	−200	BK7
D−0.051	−0.051±0.002	30	8	−192.8	−200	BK7
D−0.130	−0.130±0.002	30	8	−188.5	−200	BK7
D−0.253	−0.252±0.002	30	8	−179.9	−200	BK7

Table 2 New architecture design measurement results (tester 1).

	#1	#2	#3	#4	#5	#6
Diopters	D+0.050	D−0.130	D+0.132	D−0.051	D+0.257	D−0.252
Tolerance	±0.002	±0.002	±0.002	±0.002	±0.002	±0.002
Max.	0.052	−0.128	0.134	−0.49	0.259	−0.25
Min.	0.048	−0.132	0.13	−0.53	0.255	−0.253
Average	0.05	−0.13	0.132	−0.051	0.257	−0.252
SD.	0.0012	0.0011	0.0011	0.0011	0.0012	0.0010

Table 3 New architecture design measurement results (tester 2).

	#1	#2	#3	#4	#5	#6
Diopters	D−0.130	D−0.051	D+0.132	D−0.252	D+0.050	D+0.257
Tolerance	±0.002	±0.002	±0.002	±0.002	±0.002	±0.002
Max.	−0.128	−0.49	0.134	−0.25	0.052	0.259
Min.	−0.132	−0.53	0.13	−0.254	0.048	0.255
Average	−0.13	−0.051	0.132	−0.252	0.05	0.257
SD.	0.0011	0.0014	0.0012	0.0010	0.0013	0.0011

Fig. 10 Three pairs of goggles that had satisfactorily passed the Z87.1 test.

The measurement outcomes were assessed against the certificate of calibration reference: 2022010181/1 (stating a measurement uncertainty within ± 0.002D).[15] Each lens underwent 33 random measurements, with all resulting values falling within the allowable error range, as demonstrated in Tables 2 and 3.

The second experiment involved selecting three pairs of goggles that had satisfactorily passed the Z87.1 test. These goggles conformed to the Z87.1 acceptance standard, where the tolerance range fell within $D \pm 0.06$, as illustrated in Fig. 10.

Subsequently, two testers conducted individual tests using both the standard instrument (at a distance of 10.67 m) and the newly designed instrument. To facilitate a comparison between

Table 4 Z87.1 standard instruments (tester 1).

No.	L01-R	L01-L	Y02-R	Y02-L	IN07-R	IN07-L
Max.	0.010	0.015	−0.005	−0.005	0.025	0.007
Min.	0.000	0.005	−0.010	−0.010	0.015	0.003
Average	0.005	0.010	−0.005	−0.005	0.019	0.005
SD.	0.0032	0.0025	0.0018	0.0018	0.0006	0.0006

Table 5 New instruments (tester 1).

No.	L01-R	L01-L	Y02-R	Y02-L	IN07-R	IN07-L
Max.	0.006	0.012	−0.004	−0.004	0.020	0.006
Min.	0.004	0.010	−0.006	−0.006	0.018	0.004
Average	0.005	0.011	−0.005	−0.005	0.019	0.005
SD.	0.0006	0.0005	0.0006	0.0006	0.0006	0.0006

Table 6 Z87.1 Standard instruments (tester 2).

No.	L01-R	L01-L	Y02-R	Y02-L	IN07-R	IN07-L
Max.	0.005	0.022	−0.005	−0.005	0.035	0.015
Min.	0.000	0.010	−0.015	−0.015	0.015	0.000
Average	0.005	0.015	−0.010	−0.010	0.025	0.005
SD.	0.0024	0.0034	0.0031	0.0037	0.0047	0.0050

Table 7 New instruments (tester 2).

No.	L01-R	L01-L	Y02-R	Y02-L	IN07-R	IN07-L
Max.	0.007	0.013	−0.003	−0.003	0.021	0.007
Min.	0.003	0.009	−0.007	−0.007	0.017	0.003
Average	0.005	0.011	−0.005	−0.005	0.019	0.005
SD.	0.0012	0.0012	0.0013	0.0012	0.0011	0.0014

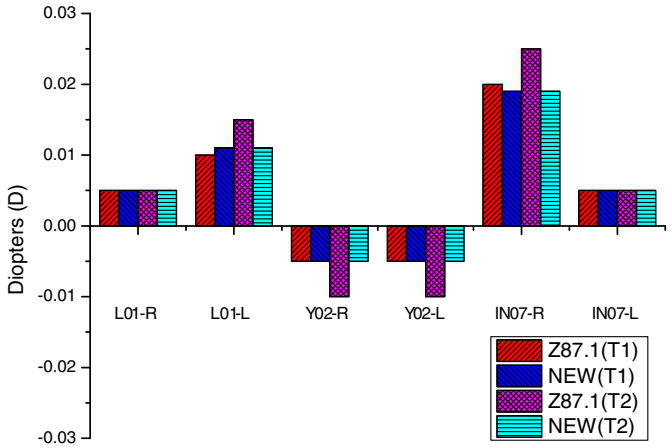

Fig. 11 The measurement results vary between the two instruments and among different personnel.

measurements, each sample underwent random measurements 33 times, and the average measurements were recorded. The resulting data from these tests is presented in Tables 4–7.

The measurement results vary between the two instruments and among different personnel as depicted in Fig. 11, within the range of $D \pm 0.01$.

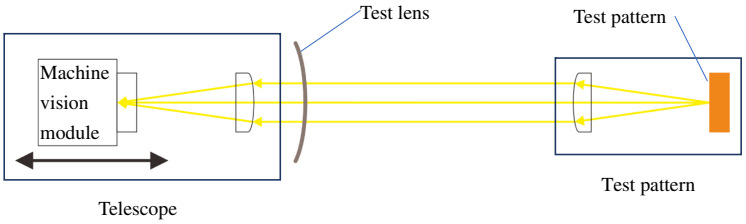

Fig. 12 Optical path diagram of the architecture.

5 Discussions

Utilizing parallel light, as illustrated in Fig. 12, the new instrument is unaffected by variations in optical path length. By integrating the optometry automatic detection instrument system depicted in Fig. 5, along with the additional space required for the measurement fixture and the correction length of the target size, the overall dimensions can be drastically reduced to <1 m.

Reducing the target size and capturing images can be affected by dust on the precision optical target, impacting the automatic interpretation of images. Hence, it is essential to assemble precision optical targets within a clean room environment to ensure the acquisition of dust-free images. Moreover, to prevent interpretation errors caused by excessive lines, the radial sunburst image and the clear line image should be measured separately. Upon downsizing the machine, each component can be enclosed within a sealed casing to mitigate external light influence and fluctuations in airflow, facilitating easier installation and transportation.

The second set of experimental results in this article reveals that the measurements obtained with the scaled-down new automated equipment in this study closely align with those recorded by the Z87.1 standard equipment. As depicted in Fig. 11, the automated inspection with the new equipment proves to be more accurate, attributed to the reduction of human operating errors. Furthermore, it is noteworthy that the measurement range of Z87.1 diopter is only ± 0.12D, whereas the new device in this study has an expanded measurement range, reaching up to ± 0.30D.

Despite the mentioned advantages of the new instrument, its measurement results may still be susceptible to operator errors in lens placement, such as tilt, and the quality of the sample itself, which includes factors like bubbles, distortion, aberrations, and material characteristics. It is crucial to acknowledge that the accuracy of the test results in this study relies on the specifications of six standard wafers. Consequently, the measurement accuracy for samples outside these standard wafer specifications remains uncertain.

6 Conclusion

After the actual test in this study, it has been verified that the measurement results of this new architecture design are reliable. Because the measurement laboratory needs to control the temperature and humidity of the environment, the costs will depend on the size of the space. The smaller the lab, the lower the cost. This new architectural design reduces the measurement distance from 10.67M to 0.24M and the target pattern scale to the ratio of 0.02249. When making precision optical targets, it is necessary to use the mask manufacturing technology of the semiconductor standard process, which can reduce the size of the overall equipment, not limited by the laboratory space, and save time and installation costs during installation.

Disclosures

The authors declare no conflict of interest.

Code and Data Availability

The data that support the findings of this study are available within this manuscript or from the corresponding author on reasonable request.

Acknowledgments

Authors gratefully acknowledge the experience support from the Yin-Tsung Company, Taiwan. This research has no funding or grant support.

References

1. E. Jackson, "Advantages of plano trial lenses," *Am. J. Ophthalmol.* **10**(4), 266–270 (1927).
2. Nissho Global Information Co., Ltd. (GII), "Global safety glasses market research report 2021" (2021).
3. Nissho Global Information Co., Ltd. (GII), "Sports sunglasses market: global industry trends, share, size, growth, opportunity and forecast 2022-2027," (2022).
4. ANSI/ISEA Z87.1-2020 Standard, *American National Standard for Occupational and Educational Eye and Face Protection Devices*, pp. 19–20, American National Standards Institute (2020).
5. L. Rodriguez-Saona et al., "Miniaturization of optical sensors and their potential for high-throughput screening of foods," *Curr. Opin. Food Sci.* **31**, 136–150 (2020).
6. P. Espadinha-Cruz, R. Godina, and E. M. G. Rodrigues, "A review of data mining applications in semiconductor manufacturing," *Processes* **9**(2), 305 (2021).
7. E. M. Taha, E. Emary, and K. Moustafa, "Automatic optical inspection for PCB manufacturing: a survey," *Int. J. Sci. Eng. Res.* **5**(7), 1095–1102 (2014).
8. A. A. R. M. A. Ebayyeh and A. Mousavi, "A review and analysis of automatic optical inspection and quality monitoring methods in electronics industry," *IEEE Access* **8**, 183192–183271 (2020)
9. Z. Yang et al., "Miniaturization of optical spectrometers," *Science* **371**, eabe0722 (2021).
10. R. C. Gonzalez and R. E. Woods, Chap. 11 in *Digital Image Processing*, 4th ed., p. 1024 (2018).
11. C. L. Chang et al., "The development of automatic optometry instrument based on the ANSI/ISEA Z87.1 standard," in *IEEE Instrum. and Meas. Technol. Conf.* (2012).
12. "Figure Figure G1: Example of Resolution and Figure G2: Examples of Resolution (Passing). ANSI/ISEA Z87.1-2020 Standard," *American National Standard for Occupational and Educational Eye and Face Protection Devices*, American National Standards Institute, p. 46 (2020).
13. R. Szeliski, Chap. 11 in *Computer Vision Algorithms and Applications*, Springer, p. 5 (2011).
14. W. H. Wu et al., "Optometric automatic inspection apparatus and method," The certificate number of patent: I453383 (2014).
15. F. Washer and I. Gardner, *Method for Determining the Resolving Power of Photographic Lenses*, National Institute of Standards and Technology, Gaithersburg, Maryland (2023).

Cheng-Chung Lee received his bachelor's and master's degrees in optometry from Chung Hwa University of Medical Technology, Taiwan, in 2011 and 2014, respectively. His academic interest focuses on the development of optical inspection mechanisms that applied in optometry.

Ching-Huang Lin received his PhD from the Department of Optics and Photonics of National Central University, Taiwan, in 2005. He has joined the faculty of the National Yunlin University of Science and Technology, Taiwan, since 2008, and currently serves as a professor and chairman within the Department of Electronic Engineering. His research interests are molecular images, lens design, and optical metrology.

Tai-Chuan Ko received his bachelor's degree in optometry from the College of Medical Science and Technology at Sun Yat-sen Medical University, in 2004. He acquired the advanced optometrist license in 2017. Currently, he holds the positions of assistant professor and department director in the Department of Optometry at Rende College of Healthcare Management in Miaoli County, Taiwan. He is actively engaged in biomedical and engineering research.

Chun-Feng Su received his doctorate degree in medicine from Kaohsiung Medical University in 1992. He has devoted himself to the field of ophthalmology as an ophthalmologist for many years. He is currently the director of Tainan Universal Eye Center in Taiwan. His main research focus is on the combination of modern Western medicine and traditional Chinese medicine in the treatment of ophthalmic diseases.